Available online at www.sciencedirect.com
ScienceDirect
Catalysis Today 123 (2007) 94–103
CATALYSIS TODAY
www.elsevier.com/locate/cattod

Effect of calcination temperature on the low-temperature oxidation of CO over CoO_x/TiO_2 catalysts

Won-Ho Yang [b], Moon Hyeon Kim [a,*], Sung-Won Ham [c]

[a] Department of Environmental Engineering, Daegu University, 15 Naeri, Jillyang, Gyeongsan 712-714, Republic of Korea
[b] Department of Occupational Health, Catholic University of Daegu, 330 Geumnak, Hayang, Gyeongsan 712-702, Republic of Korea
[c] Department of Display and Chemical Engineering, Kyungil University, 33 Buho, Hayang, Gyeongsan 712-701, Republic of Korea

Available online 26 February 2007

Abstract

A 5 wt% CoO_x/TiO_2 catalyst has been used to study the effect of calcination temperature on the activity of this catalyst for CO oxidation at 100 °C under a net oxidizing condition in a continuous flow type fixed-bed reactor system, and the catalyst samples have been characterized using TPD, XPS and XRD measurements. The catalyst after calcination at 450 °C gave highest activity for this low-temperature CO oxidation, and XPS measurements yielded that a 780.2-eV Co $2p_{3/2}$ main peak appeared with this catalyst sample and this binding energy was similar to that measured with pure Co_3O_4. After calcination at 570 °C, the catalyst, which had possessed practically no activity in the oxidation reaction, gave a Co $2p_{3/2}$ main structure peak at 781.3 eV which was very similar to those obtained for synthesized Co_nTiO_{n+2} compounds ($CoTiO_3$ and Co_2TiO_4), and this catalyst sample had relatively negligible CO chemisorption as observed by TPD spectra. XRD peaks indicating only the formation of Co_3O_4 particles on titania surface were developed in the catalyst samples after calcination at temperatures ≥350 °C. Based on these characterization results, five types of Co species could be modeled to exist with the catalyst calcined at different temperatures. Among these surface Co species, the Type A clean Co_3O_4 particles were predominant on a sample of the catalyst after calcination at 450 °C and highly active for CO oxidation at 100 °C, and the calcination at 570 °C gave the Type B Co_3O_4 particles with complete Co_nTiO_{n+2} overlayers inactive for this oxidation reaction.

Keywords: CO oxidation; TiO_2-supported cobalt oxides; Calcination temperature effect; Co_3O_4; Cobalt titanates; X-ray photoelectron spectroscopy (XPS)

1. Introduction

Catalytic CO oxidation at low temperatures has been one of the most common topics in many environmental and industrial applications such as engine-out emissions control for advanced vehicles with homogeneous charge compression ignition (HCCI) engines, reformer product purification for polymer electrolyte fuel cells, indoor air cleaning, gas sensors, gas masks and prevention of the deactivation of CO_2 lasers [1–8]. Among the current and future widespread use of low-temperature CO oxidation in such applications, the former two cases are of particular interest because of the potential utilization of the low-temperature oxidation processes not only to selectively (preferentially) remove CO existing with excess H_2 at the outlet of a steam reformer and multi-staged water gas shift reactor for fuel cells, but also to significantly lower CO in exhaust gases from HCCI combustion engines.

Hydrogen-fuelled polymer electrolyte membrane fuel cells, representatively proton-exchange membrane fuel cells (PEMFCs), have been recognized to be the most environmentally benign energy conversion system for road vehicle applications in the near future [9–11]. The on-board production of H_2 from less explosive gaseous or liquid hydrocarbons using a systematic combination of catalytic steam reforming processes with a water–gas shift reaction needs to overcome some technical barriers associated with the distribution and storage of H_2 for commercialization of the fuel cell systems. However, the reformer gas products contain large amounts of CO (typically 0.5–2% as compiled in Table 1) by which anodic Pt electrocatalysts in the fuel cell systems are known to be significantly deactivated [12,13]. In an attempt to lower CO in H_2-rich gas streams to acceptable levels less than 100 ppm [12,14], preferential oxidation (designated to ''PrOx'') of CO has been extensively studied using a variety of catalysts that

* Corresponding author. Tel.: +82 53 850 6693; fax: +82 53 850 6699.
E-mail address: moonkim@daegu.ac.kr (M.H. Kim).

0920-5861/$ – see front matter © 2007 Elsevier B.V. All rights reserved.
doi:10.1016/j.cattod.2007.01.048

Table 1
Simulated conditions for PEMFC and HCCI vehicle applications [11–14,17,22]

Gas compositions and operating temperature window	PEMFC	HCCI
CO (%)	0.5–2	>1
H_2 (%)	45–75	n.d.
CO_2 (%)	15–25	n.d.
H_2O (%)	15–30	n.d.
NO_x (ppm)	n.d.	<20
HC (%)[a]	Trace	>1
PM (mg/m^3)	n.d.	≈0[b]
T (°C)	70–300	r.t.–280

Note. n.d. = no data; r.t. = room temperature.
[a] Unconverted or unburned.
[b] Under detection limits.

must possess high activity and selectivity in the temperature range of 70–300 °C because the PrOx catalysts are placed between the reformer and the fuel cell system operated at the respective temperatures ranging from 70–130 to 200–300 °C [11–13,15].

The HCCI combustion has been proposed to be an alternative and attractive technology for internal combustion engines that can offer a great potential of high thermal efficiencies, comparable to or greater than conventional diesel engine vehicles, and dramatic reduction in NO_x ($NO + NO_2$) and particulate matter (PM) emissions [1,16,17]; therefore, HCCI engine-equipped automobiles are probably one of the most promising candidates to meet very stringent future emission standards, e.g., Tier 2 program in the United States and EURO 5 in Europe. One of the current challenges to the HCCI technology for road applications is to control CO and unburned hydrocarbons (HCs) emissions with concentrations greater than 1% as seen in Table 1. These emissions occur at low exhaust temperatures that make it difficult to employ catalysts, such as well-proven three-way catalytic converters (TWCs), for reducing the engine-out emissions [18]. Furthermore, the TWCs consisting of Rh, Pt and Pd as major active moieties would not be available for HCCI applications because of high concentrations of O_2 in the exhaust which can readily transform the Rh to an inactive Rh_2O_3 [2,19,20]. This also motivates the development of new catalysts for low-temperature CO oxidation under oxidizing conditions.

Supported precious noble metals, such as Pt, Rh, Pd, Ru, and Ir, have been well-known catalysts for low-temperature CO oxidation with high performances and stability [8,9,12,15,21–25], and are widely employed as key constituents in automotive catalysts for engine-out emissions control. Since Haruta et al. [26] reported very high activity for CO oxidation even at temperatures as low as −70 °C over nanosized gold particles (<10 nm) dispersed uniformly on transition metal oxides, representatively Co_3O_4, Fe_2O_3 and NiO, supported Au nanoparticles have received a great attention for the oxidation of CO at low temperatures under purely oxidizing and PrOx conditions [8–10,27–29]. However, the need to substitute for the supported platinum group metals-based and Au catalysts is because of the high cost of precious metals and their weak sulfur tolerance [30–35]. For this purpose, a huge body of candidates have been proposed for low-temperature CO oxidation to date and there exist very promising catalysts for the PEMFC and HCCI applications, depending on their preparation techniques, activation protocols and testing conditions. Supported or promoted CuO systems have been studied as substitute catalysts for low-temperature CO oxidation [6–8,11,13,14,23,36,37], and CuO–CeO_2 mixed oxides are highly active and exceptionally selective for the oxidation reaction with a simulated PrOx condition. Recently, Pillai and Deevi [38] have reported unpromoted and unsupported CuO that was obtained via a precipitation method following an activation process in flowing O_2/CO, and this catalyst gives complete CO oxidation even at ambient temperature. Another alternative to the precious metals may be unsupported and supported cobalt oxides, and these catalysts have been well known to be quite active for CO oxidation at very low temperatures [4,26,39–44]. Unsupported Co_3O_4 powders possess high, reproducible activity for catalytic CO oxidation at temperatures greater than 150 °C, depending significantly on calcination temperatures used, although the rate of the CO conversion could decrease in the presence of HCs, NO, and H_2O [40]. A similar observation is reported by Teng et al. [43] who yielded 100% CO conversion at 150 °C with unsupported Co_3O_4 even in the presence of excess H_2. However, much higher performance, based on temperatures exhibiting 100% CO conversion, is indicated for a pure Co_3O_4 catalyst, obtained via the calcination of precipitated cobalt carbonates at 400 °C, on which complete CO conversion around −50 °C occurs when a CO–O_2 reaction mixture was specially dehumidified [44]. Cobalt oxides dispersed on Al_2O_3, SiO_2, MgO, La_2O_3, CeO_2, and $SrCO_3$ have been frequently used for the oxidation of CO at low temperatures [42,45–51], and it is shown that the extent of catalytic CO conversion in the oxidation reaction depends on the supports and pretreatment procedures used.

As seen in Table 1, one of the noteworthy differences in conditions between PEMFC and HCCI applications is the high concentration of H_2. Co_3O_4 gave no activity for H_2 oxidation at low temperatures, such as 130 °C, when using a flowing mixture of CO, H_2 and O_2 in N_2 [52]. Compared to the CoO_x dispersed on SiO_2 and Al_2O_3, CoO_x/TiO_2 catalysts were very difficult to reduce while flowing pure H_2, even at 300 °C [39]. This suggests CoO_x species that are active for CO oxidation at low temperatures, e.g., Co_3O_4, may be much more stable on TiO_2 surfaces, even in the presence of H_2. Although low-temperature CO oxidation reactions under net oxidizing and simulated PrOx conditions have been examined on the supported CoO_x catalysts [42,45–51], we could find only one study of TiO_2-supported CoO_x catalysts for CO oxidation at low temperatures. This earlier study by Epling et al. indicated that after calcination at 500 °C a CoO_x/TiO_2 catalyst is active for CO oxidation at temperatures ranging from 130 to 180 °C under a PrOx condition [53]. This study reports significant differences in CO oxidation activity at low temperatures between TiO_2-supported CoO_x catalysts calcined at different temperatures. These CoO_x/TiO_2 samples were characterized via TPD, XPS and XRD measurements to clarify such remarkable dependence of the catalytic activity on the calcination excursion. This effort

reported here is not intended to be a comprehensive study on the effects of H_2, HCs, CO_2, and H_2O on the catalytic performances of this CO oxidation reaction, as these will be covered in another study.

2. Experimental

2.1. Catalyst preparation

Rod-type TiO_2, which was received from Millennium Chemicals (DT51D) and consists of pure anatase structure with a specific surface area of 38 m^2/g, was employed to prepare a supported CoO_x catalyst. Prior to dispersing the CoO_x onto the TiO_2, it was powdered and calcined at 570 °C for 4 h in flowing air (Praxair, 99.999%) at 1000 cm^3/min. CoO_x/TiO_2 catalyst containing 5 wt% CoO_x based on the Co element was obtained by incipient wetness in which an aqueous solution of $Co(NO_3)_2{\cdot}6H_2O$ (Aldrich, 99.999%) was impregnated dropwise, as described elsewhere [54,55]. After the simple impregnation, this catalyst was dried in air overnight at 110 °C and stored in a desiccator for later use.

Cobalt titanates such as $CoTiO_3$ and Co_2TiO_4 were synthesized via the following solid-state reaction at high temperatures:

$$CoO + TiO_2 \rightarrow CoTiO_3 \quad (1)$$

$$2CoO + TiO_2 \rightarrow Co_2TiO_4 \quad (2)$$

To obtain the $CoTiO_3$ according to Eq. (1), a stoichiometric amount of the TiO_2 and CoO (Aldrich, 99.99+%) was thoroughly mixed using a mortar and pestle. An appropriate amount of the solid mixture (ca. 2.3 g) was loaded into a laboratory-designed I-shaped quartz reactor and treated at 1150 °C for 6 h under a flow of pure air at 100 cm^3/min. The Co_2TiO_4 was produced in a way similar to that described for the $CoTiO_3$ synthesis, and these samples were employed for instrumental measurements and low-temperature CO oxidation later.

2.2. Catalytic CO oxidation

Each activity profile for CO oxidation at 100 °C over 5 wt% CoO_x/TiO_2 samples after calcination at different temperatures was obtained using a continuous flow fixed-bed type U-shaped Pyrex reactor with a 1/4-in. o.d. inlet and outlet and 3/8-in. o.d. catalyst bed placed in a bottom-capped cylindrical electric furnace coupled with a PID temperature controller (Hanyoung NP200). Typically 0.4 g catalyst was placed above a quartz wool plug in the Pyrex reactor and routinely calcined at 350, 450 or 570 °C for 1 h *in situ* in flowing air at 100 cm^3/min using a Brooks 5850E mass flow controller, prior to being used for the catalytic oxidation of CO (Matheson, 99.99%). The air was purified by flowing it through an Alltech moisture trap.

A typical gas mixture consisting of 1% CO and 3% O_2 in flowing He (Praxair, 99.999%) at a total flow rate of 100 cm^3/min, corresponding to a gas hourly space velocity (GHSV) of 6000 h^{-1}, was passed over the catalyst bed for CO oxidation at 100 °C. All the gas flow rates during on-stream activity measurements were controlled using Brooks 5850E and MKS Type 1179A mass flow controllers. The effluent gases were analyzed using an on-line, computer-controlled Agilent 6890N gas chromatograph equipped with a thermal conductivity detector and a Porapak Q column and a molecular sieve 13× column (Alltech Assoc.) for the respective CO_2 and CO separations, and the CO_2 concentration produced was used for verifying the mass balance. The extent of the conversion of CO during the oxidation reaction was evaluated based on CO concentrations in the up- and downstream.

2.3. Characterization via TPD, XRD and XPS

The 5 wt% CoO_x/TiO_2 catalyst was calcined in flowing air for 1 h at different temperatures – 250, 350, 450, and 570 °C – prior to X-ray diffraction (XRD) measurements. Reference Co compounds such as Co_3O_4, $Co(OH)_2$ (Aldrich, 95%) and CoO were used as-received for XRD measurements. XRD spectra of all these samples were collected *ex situ* using a Rigaku D/MAX2500 PC diffractometer equipped with a Cu Kα (λ = 1.54056 Å) radiation source and a graphite monochromator. The respective X-ray tube voltage and current during the data collection were 40 or 100 kV and 20 mA. Each sample was loaded onto a thin quartz holder with a 12 mm diameter in the diffractometer and scanned from a 2θ value of 10° to 80° at a normal scanning rate of 2.0°/min. Subsequently, a high resolution scanning rate of 0.1°/min was allowed to obtain more accurate peaks of Co_3O_4 in the catalyst samples calcined at each temperature, and average crystallite sizes for the Co_3O_4 were determined based on linewidth at half height of the XRD peak at $2\theta = 31.26°$ by the crystallographic (2 2 0) plane using the Scherrer equation with Warren's correction for instrumental line broadening. XRD patterns for $CoTiO_3$ and Co_2TiO_4 samples synthesized here were compared to those of the corresponding standard PDF files # 77-1373 and 39-1410 to acquire successful synthesis of these cobalt titanates.

X-ray photoelectron spectroscopy (XPS), using a VG Scientific ESCALAB 220-IXL X-ray photoelectron spectrometer with an unmonochromatized Mg Kα photon source having a radiation energy of 1253.6 eV, was employed to obtain Co 2p energy spectra for 5 wt% CoO_x/TiO_2 calcined at the four different temperatures. These XPS spectra were compared to those obtained with the reference Co compounds used for XRD measurements to determine surface chemical oxidation states of Co species produced in the catalyst samples. An appropriate amount (ca. 10 mg) of each sample was loaded into a pelletizer with a 10 mm diameter and pressed to obtain a homogeneous, thin self-supporting wafer, as described earlier [56]. Prior to transferring each sample disk into the instrument to give a dynamic vacuum below 10^{-10} Torr (1 Torr = 133.3 Pa), it was dried and degassed in the prevacuum chamber for 2 h. All Co 2p XPS spectra for the samples were recorded with a scan number of 10 and corrected using the C 1s peak at 284.8 eV.

In situ TPD (temperature programmed desorption) spectra of CO adsorbed at 50 °C on 5 wt% CoO_x/TiO_2 after calcination at either 450 or 570 °C were collected using an on-line, computer-controlled OmniStar GSD 301 O2C quadruple mass

spectrometer (Pfeiffer Vacuum Technology) coupled with a laboratory-designed TPD cell placed in an electric furnace. A feed gas handling system and temperature controller were combined with this TPD system to allow *in situ* sample pretreatments. After loading a 50 mg sample in the TPD cell, it was calcined in a fashion similar to that used for the activity measurements and cooled down to 50 °C at which the sample was exposed to 1% CO in He at a flow rate of 30 cm^3/min for 30 min. After purging the TPD cell with pure He for 2 h, it was heated to 400 °C at a rate of 10 °C/min under 30 cm^3 (STP)/min of pure He for desorbing the CO from the catalyst surface. During each experiment, the CO desorption was monitored at 28 amu. All gases used were purified as described above.

3. Results

Activity profiles of the 5 wt% CoO_x/TiO_2 catalyst calcined at 350, 450 and 570 °C for CO oxidation at 100 °C are shown in Fig. 1 with bare TiO_2. The supported CoO_x catalyst after calcination at 350 °C had a 38% CO conversion when measured after 4 min on stream; this conversion was stable for 2 h. Calcining the catalyst at 450 °C gave CO conversions near 82%, which was much higher than the catalyst calcined at 350 °C. Surprisingly, CO conversions were below 2% for all on-stream hours allowed, when the catalyst was calcined at 570 °C. The bare TiO_2 used as the support was shown to be completely inactive for this low-temperature CO oxidation reaction, in good agreement with earlier results [53,57]. All CO conversions were consistent with CO_2 production rates during the oxidation reaction. In an independent measurement of the activity for CO oxidation with 5 wt% CoO_x/TiO_2 after calcination at 450 °C, this catalyst had stable conversions around 80% even after 18 h on stream (not shown).

To provide a direct measurement of the effect of calcination temperature on 5 wt% CoO_x/TiO_2, a single sample of this catalyst was first calcined at 450 °C *in situ* in the reactor before

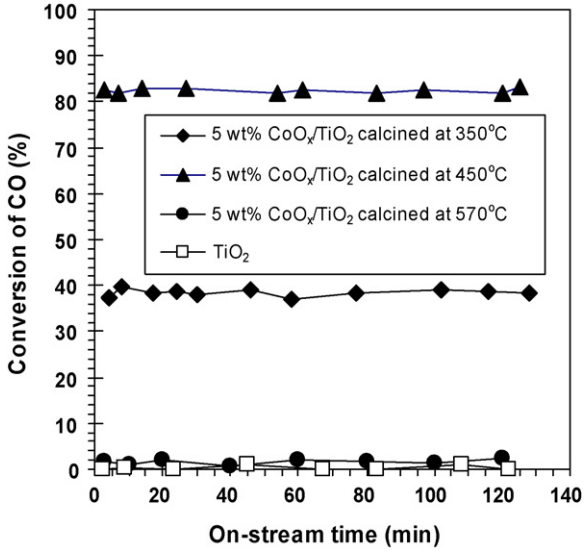

Fig. 1. Activity profiles for CO oxidation at 100 °C over 5 wt% CoO_x/TiO_2 calcined at 350, 450 and 570 °C.

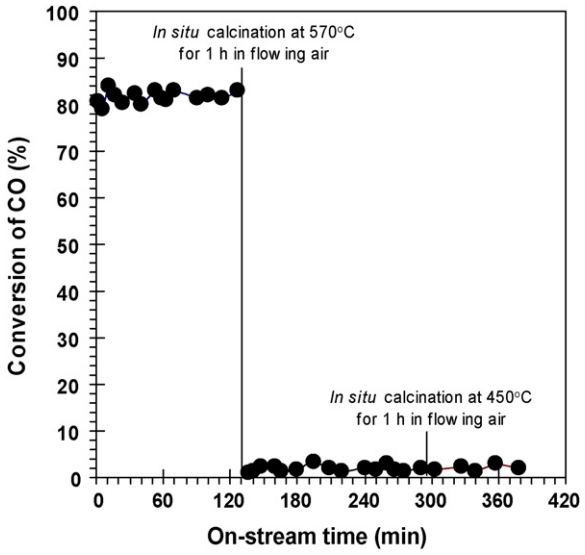

Fig. 2. Catalytic activity for CO oxidation at 100 °C over 5 wt% CoO_x/TiO_2 after *in situ* calcination at 450 °C followed by consecutive calcination at 570 and 450 °C. The vertical solid bars differentiate the three calcination steps.

CO oxidation at 100 °C, and then the sample was subjected to consecutive calcination at 570 and 450 °C following the CO oxidation. About 82% CO conversion was again achieved after the 450 °C calcination and maintained for ~2 h, as demonstrated in Fig. 2. If this sample was calcined at the higher temperature, the conversion decreased to around 2% which was the case with the earlier sample in Fig. 1; this observation was irreversible. Thus it is clear that the activity of this TiO_2-supported CoO_x catalyst for CO oxidation at 100 °C depended strongly on calcination temperature.

Fig. 3 shows *in situ* TPD spectra for 5 wt% CoO_x/TiO_2 after calcination at either 450 or 570 °C following exposure to a flow of 1% CO in He at 50 °C. The sample calcined at 450 °C possessed an intense CO desorption peak at 143 °C along with a weak shoulder at 216 °C, as displayed in Fig. 3a. This main desorption peak position had a higher temperature, by 80 °C, than that reported by Thormahlen et al. [42], but their CoO_x/Al_2O_3 catalyst was calcined at 550 °C for 1 h and subsequently reduced at 627 °C for 10 min. The spectrum for CO desorbed from the catalyst, which had been calcined at 570 °C, gave a very weak peak at 87 °C (Fig. 3b). In either case, no CO desorption peaks appeared at temperatures above 250 °C.

The powder XRD pattern of 5 wt% CoO_x/TiO_2 calcined at 450 °C, which had given the highest on-stream performance in CO oxidation at 100 °C, was taken to identify crystalline phases for the CoO_x species present in this catalyst and compared to those of the reference Co compounds and of a sample of 5 wt% CoO_x/TiO_2 after calcination at 250, 350 and 570 °C, and all these XRD spectra are provided in Figs. 4 and 5. An original intensity of the XRD patterns for the samples was reduced, by 60 or 95%, to give an easier comparison; however, all characteristic peaks were clearly visible even after such reduction. The $Co(OH)_2$ sample gave the most intense diffraction peak at $2\theta = 19.04°$ with substantial reflections at higher 2θ values, as shown in Fig. 4c. Diffraction patterns, taken

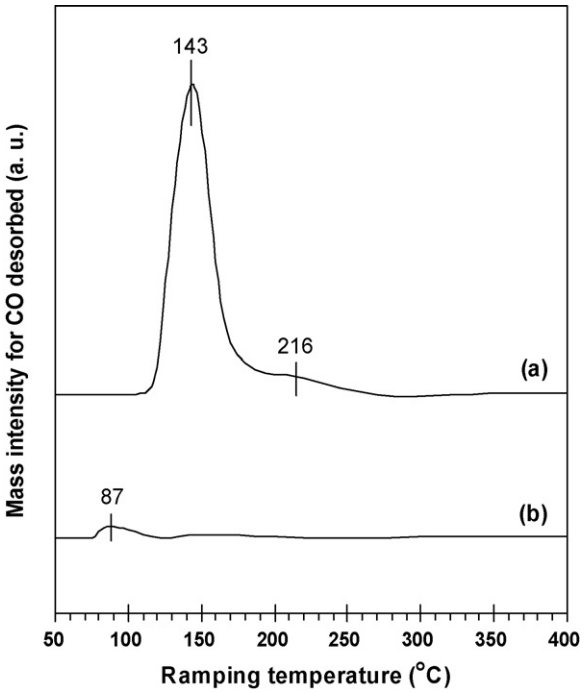

Fig. 3. *In situ* TPD spectra for CO desorbed from the surface of 5 wt% CoO_x/TiO_2 after calcination at: (a) 450 °C and (b) 570 °C. After CO adsorption at 50 °C on each sample, a 2 h purge with He was allowed prior to being heated up to 400 °C.

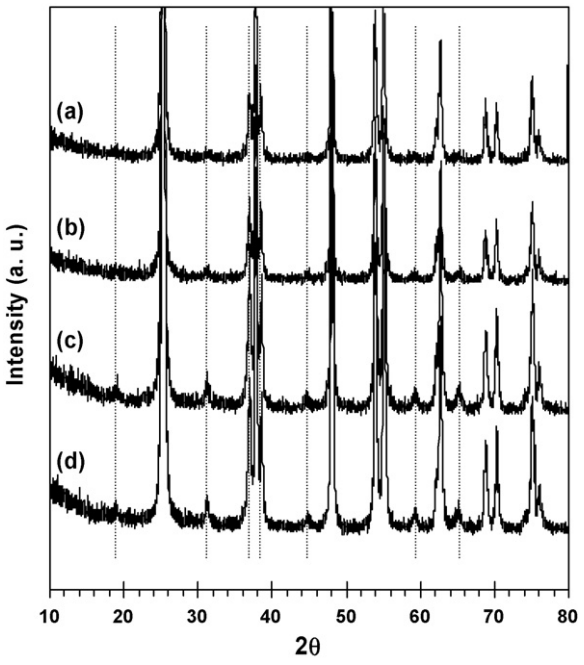

Fig. 5. XRD patterns for 5 wt% CoO_x/TiO_2 after calcination at: (a) 250 °C; (b) 350 °C; (c) 450 °C; (d) 570 °C. The vertical dotted bars represent the diffraction lines for Co_3O_4.

with the reference Co_3O_4 sample, occurred at 2θ values of 18.99°, 31.26°, 36.84°, 38.56°, 44.80°, 59.38° and 65.22°, and the 36.84° peak concerning with the crystallographic (3 1 1) plane of Co_3O_4 was predominant (Fig. 4d). XRD measurement

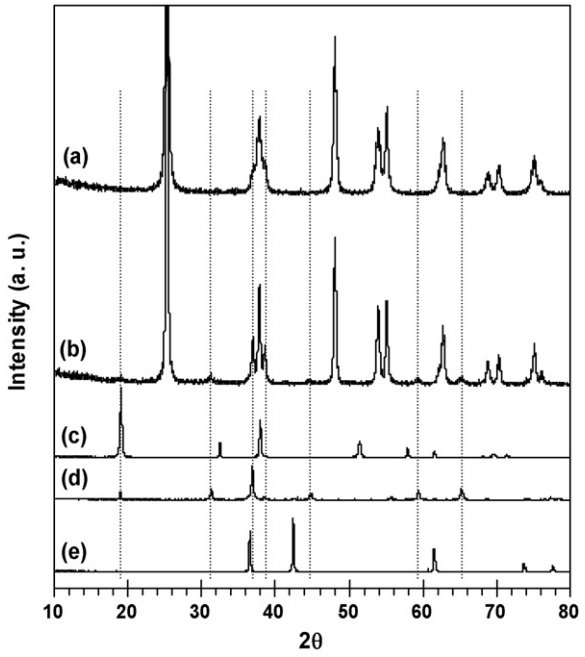

Fig. 4. XRD patterns for reference Co compounds, and 5 wt% CoO_x/TiO_2 calcined at 450 °C: (a) TiO_2; (b) 5% CoO_x/TiO_2 calcined at 450 °C; (c) $Co(OH)_2$; (d) Co_3O_4; (e) CoO. The vertical dotted bars represent the diffraction peaks for Co_3O_4.

with the reference CoO yielded two intense peaks at $2\theta = 36.56°$ and 42.42° with three weak peaks at $2\theta = 61.54°$, 73.78° and 77.67° (Fig. 4e). The pure anatase TiO_2 showed a predominant characteristic peak at a 2θ value of 25.30°, corresponding to the (1 0 1) crystalline plane, with substantial reflections at higher 2θ values (Fig. 4a). Additional diffraction peaks by the presence of CoO_x species in the TiO_2-supported catalyst after calcination at 450 °C appeared at 2θ values of 18.98°, 31.19°, 36.92°, 38.58°, 44.79°, 59.37° and 65.22°, as indicated by the vertical dotted bars in Fig. 4b, and these XRD peak positions were almost equal to that revealed for Co_3O_4 in Fig. 4d.

XRD spectra for 5 wt% CoO_x/TiO_2 after calcination at 250, 350 and 570 °C are shown in Fig. 5 in which the preceding pattern of the catalyst calcined at 450 °C has been again included to readily allow a comparison. As calcination temperature increased up to 450 °C, the XRD peaks associated with Co_3O_4 became developed, as seen in Fig. 5a–c, but all the indicated peaks were no longer intensified even after calcination at 570 °C. There were no discernable CoO peaks, irrespective of calcination temperature. The Co_3O_4 existing with the catalyst after calcination at 450 °C indicated a crystallite size of 29 nm, based on the 31.26° peak corresponding to the (2 2 0) plane, and a very similar particle size for Co_3O_4 could be obtained even with a sample of the catalyst calcined at 570 °C. Based on these XRD measurements, it is shown that all the catalyst samples calcined at 450 and 570 °C consisted of Co_3O_4 nanoparticles, although these two samples gave the noticeable difference in activity for the low-temperature CO oxidation as discussed previously.

Co 2p XPS spectra of 5 wt% CoO_x/TiO_2 following calcination at different temperatures are shown in Fig. 6. The

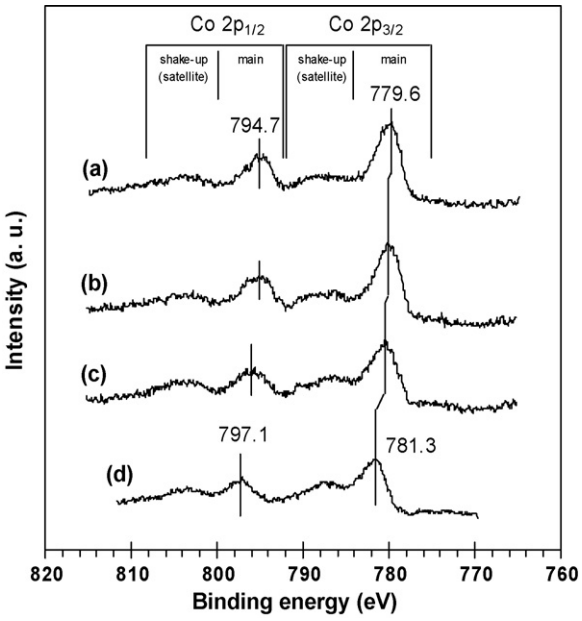

Fig. 6. Co 2p XPS spectra for 5 wt% CoO_x/TiO_2 after calcination at: (a) 250 °C; (b) 350 °C; (c) 450 °C; (d) 570 °C.

spectral features of samples of the catalyst calcined at 450 and 570 °C were of particular interest to us because of the need to reasonably understand the remarkable difference in activity between these samples during CO oxidation reaction at 100 °C. A main peak of Co $2p_{3/2}$ at a binding energy of 779.6 eV was visible with a Co $2p_{1/2}$ main peak at 794.7 eV for the catalyst calcined at 250 °C (Fig. 6a), while the calcination at 350 °C gave a slightly higher binding energy by 0.2 eV (Fig. 6b). When the catalyst was calcined at 450 °C, a main peak at 780.2 eV was observed for Co $2p_{3/2}$ (Fig. 6c). Calcination of the CoO_x catalyst at 570 °C gave a Co $2p_{3/2}$ main structure at a binding energy of 781.3 eV, along with a main peak at 797.1 eV for Co $2p_{1/2}$ (Fig. 6d). It is clear that the maxima of Co 2p main peaks were shifted to higher binding energies as calcination temperature increased, and that the sample calcined at 570 °C had significantly higher Co 2p binding energies, by 1.1 and 2.4 eV for the respective Co $2p_{3/2}$ and Co $2p_{1/2}$, than that measured after calcination at 450 °C. The 781.3 eV binding energy for Co $2p_{3/2}$ main structure was very similar to those reported earlier for $CoTiO_3$ and Co_2TiO_4 [58]; thus, this strongly suggests the formation of such cobalt titanates in the sample calcined at 570 °C. All these binding energy values for Co $2p_{3/2}$ are listed in Table 2.

XRD patterns for $CoTiO_3$ and Co_2TiO_4 synthesized to directly measure their Co 2p binding energies and time-on-stream performances in the oxidation of CO at 100 °C are shown in Fig. 7. The two cobalt titanates indicated 2θ peak positions which were identical to those based on the respective JCPDS references, and the relative intensity of major characteristic peaks in each sample synthesized was consistent with that observed in each corresponding JCPDS XRD spectrum. These XRD results confirmed successful synthesis of the cobalt titanates. Finally, when these cobalt titanates were used for CO oxidation at 100 °C, none of them were active for this reaction because of giving less than 1% CO conversion for 2 h (not shown).

Table 2
Binding energies for Co $2p_{3/2}$ in 5 wt% CoO_x/TiO_2 and reference Co compounds

Sample	Calcination temperature (°C)	Binding energy (eV)
CoO_x/TiO_2	250	779.6
CoO_x/TiO_2	350	779.8
CoO_x/TiO_2	450	780.2
CoO_x/TiO_2	570	781.3
$CoTiO_3$	n.d.	781.3
Co_2TiO_4	n.d.	781.1
CoO	n.d.	780.3
CO_3O_4	n.d.	779.9
$Co(OH)_2$	n.d.	781.2

Note. n.d. = no data.

Co 2p XPS spectra of the reference Co compounds were collected to determine the surface chemical states of the CoO_x species existing with 5 wt% CoO_x/TiO_2 after calcination at different temperatures, and these reference XPS spectra are provided in Fig. 8. The $CoTiO_3$ sample gave two main peaks at binding energies of 781.3 and 797.3 eV for the respective Co $2p_{3/2}$ and Co $2p_{1/2}$ with each corresponding satellite peak at higher energies, while Co 2p main structure peaks in Co_2TiO_4 appeared at slightly lower binding energies by 0.2 eV. These binding energy values for Co $2p_{3/2}$ were very similar to that documented in the literature [58]. The CoO reference was characterized by main peaks at 780.3 and 796.2 eV with discernable satellites at higher binding energies, which is consistent with earlier XPS results for CoO [59,60]. A Co $2p_{3/2}$ main peak at 779.9 eV was observed for the reference Co_3O_4. The $Co(OH)_2$ sample possessed a predominant peak at

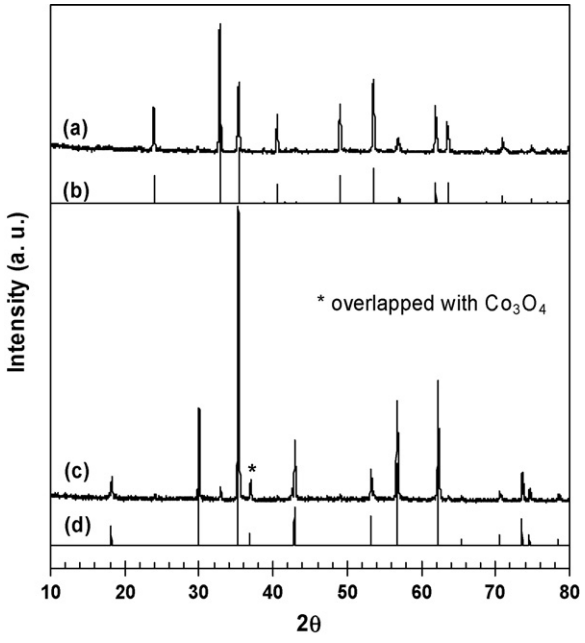

Fig. 7. XRD patterns for synthesized $CoTiO_3$ and Co_2TiO_4 compounds: (a) $CoTiO_3$ synthesized; (b) JCPDS # 77-1373 for reference $CoTiO_3$; (c) Co_2TiO_4 synthesized; (d) JCPDS # 39-1410 for reference Co_2TiO_4.

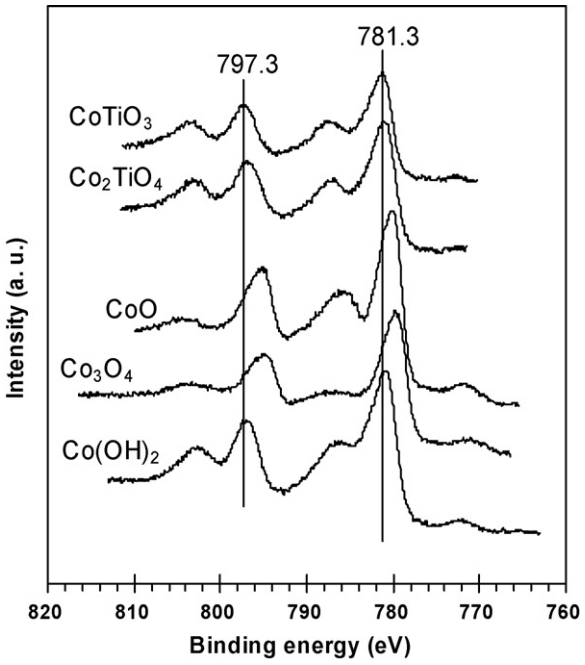

Fig. 8. Co 2p XPS spectra for reference Co compounds.

781.2 eV for Co $2p_{3/2}$ with an intense satellite structure, in good agreement with that obtained by Sexton et al. [59]. All these XPS results are also listed in Table 2 to allow a comparison between main structure binding energies for Co $2p_{3/2}$.

4. Discussion

Cobalt-based catalysts dispersed on porous solid materials, such as SiO_2, Al_2O_3, and TiO_2, are widely used for industrial Fischer–Tropsch synthesis processes, and relatively high-temperature calcination of these supported cobalt catalysts following reduction is usually required to obtain a metallic Co that is active for the synthesis reaction [61]. Except for Co_3O_4 and CoO formation, different Co species, e.g., Co_2SiO_4, $CoAl_2O_4$, $CoAlO_4$, and $CoTiO_3$, can be produced by a change in the metal–support interface due to the strong metal–support interaction (SMSI) during the calcination. Depending on the activation temperature, the acidic properties of supports and their porous structure, the composition of reducing agents and so forth, these cobalt-support species are inactive for the synthesis reaction and are very stable such that they are reducible only at temperatures greater than 500 °C [58,61–63]. Such inactive Co phases are more easily formed on Al_2O_3 and TiO_2, compared to SiO_2. It is well known that SiO_2 is an excellent adsorbent for H_2O; therefore, this support may not be suitable for the highly humid conditions given in Table 1. TiO_2, however, has a relatively strong tolerance to H_2O and CO_2 [64,65]. XPS measurements allow us to differentiate chemical oxidation states of surface Co species present in supported Co catalysts. This is due to the significant differences between Co 2p binding energies of each Co species in the XPS spectra, which usually consist of a main peak accompanied by an adjacent shake-up structure; however, XPS data are obtained within approximately 20 atomic layers close to the surface and can be significantly different from that in the entire sample [66]. This surface-sensitive data can be supplemented with XRD measurements to analyze the bulk-phase structure.

The time-on-stream activity of 5 wt% CoO_x/TiO_2 for the catalytic oxidation of CO at 100 °C under a purely oxidizing condition depends dramatically on temperatures to calcine this catalyst, and the range of indicated CO conversions is practically 0–82%, as given in Fig. 1. Although unsupported Co_3O_4 powders for CO oxidation at ambient temperature had a gradual decrease in activity with time [4,44,46], the supported CoO_x catalyst exhibits no deactivation for at least 2 h, irrespective of calcination temperature. Among CoO_x/TiO_2 samples calcined at different temperatures, the catalyst calcined at 450 °C has the highest activity for CO oxidation reaction at 100 °C and is much more active than earlier reported Co/Al_2O_3 catalysts that were calcined at 500 °C for 2 h and subsequently reduced at temperatures ranging from 350 to 450 °C in a flow of pure H_2 [45,51,67]. However, almost zero activity is observed with the catalyst following calcination at 570 °C for all operating hours. If a sample of 5 wt% CoO_x/TiO_2 calcined first at 450 °C is calcined at 570 °C, it has very low CO conversions near zero (Fig. 2), suggesting that active CoO_x species existing after calcination at 450 °C may be irreversibly altered to an inert Co phase upon the higher temperature calcination. Negligible CO chemisorption was observed on the inactive Co catalysts, as observed by *in situ* TPD spectra in Fig. 3. Consequently, the dramatic effect of the calcination temperature on the activity in this low-temperature CO oxidation over 5 wt% CoO_x/TiO_2 is associated with the formation of inactive Co-containing species by the SMSI effect.

The XRD results given in Figs. 4 and 5 readily provide the bulk-phase structure of the CoO_x species present in samples of 5 wt% CoO_x/TiO_2 following calcination at four different temperatures. When the XRD patterns of these samples are compared to those for the reference Co compounds, the catalyst after calcination at 250 °C shows no CoO_x peaks, but the remaining samples all exhibit CoO_x diffraction lines that correspond to Co_3O_4. Neither CoO nor Co_nTiO_{n+2} ($CoTiO_3$ and Co_2TiO_4) is indicated for all these samples. Among all the diffraction peaks for the synthesized Co_nTiO_{n+2} compounds shown in Fig. 7, only a small peak at a 2θ value of 36.88° (Fig. 7c) is overlapped with for a peak for Co_3O_4. Characterization of samples of 5 wt% CoO_x/TiO_2 after calcination at different temperatures by acquiring XPS spectra of the Co 2p core levels can be used to distinguish between surface chemical states of the CoO_x species active for the oxidation of CO at 100 °C. The reference Co_3O_4 has a weak satellite structure for Co $2p_{3/2}$ because of the presence of both magnetic Co^{2+} ions and diamagnetic low-spin Co^{3+} ions located in the respective tetrahedral (T_d) and octahedral (O_h) coordination sites [68,69], while the reference CoO gives a very strong Co $2p_{3/2}$ shake-up peak due to the presence of only Co^{2+} ions occupying the O_h sites (Fig. 8). Thus, it is not difficult to differentiate the Co $2p_{3/2}$ spectral difference between these two Co species. Not only are the binding energies for Co 2p in the reference cobalt titanates synthesized here significantly higher

than those measured with CoO and Co_3O_4, by 0.8–1.4 eV, but stronger Co $2p_{3/2}$ satellite structures are also represented for these references possessing Co^{2+} cations alone, as compared to Co_3O_4 (Fig. 8 and Table 2). The Co $2p_{3/2}$ binding energy values for the synthesized Co_nTiO_{n+2} compounds are very similar to those reported earlier for $CoTiO_3$ and Co_2TiO_4 [58].

Pure Co compounds, such as CoO, Co_3O_4, Co_2TiO_4 and $CoTiO_3$, and TiO_2-supported CoO_x catalysts have been studied by XPS, NIR and XRD measurements [58–60,70–73]. Based on these earlier results, the Co $2p_{3/2}$ main structure peaks observed for 5 wt% CoO_x/TiO_2 after calcination at different temperatures can be assigned, i.e., 779.8, 780.2 and 781.3 eV (Table 2). The 780.2 eV peak in a sample of the catalyst calcined at 450 °C is indicative of the presence of Co_3O_4 [60,70]. This peak has a binding energy very similar to that obtained with CoO (Table 2) but may not be associated with the CoO because no XRD peaks were observed for CoO in the sample calcined at 450 °C (Fig. 5c); furthermore, the formation of Co_3O_4 is typical on supports when calcining Co precursor salts at high temperatures in oxygen [62,72]. The reason why this catalyst sample gave somewhat higher binding energy for the Co $2p_{3/2}$ main peak than that measured with pure Co_3O_4 is probably due to a weak SMSI effect [73]. This can be supported by the 779.8 eV binding energy (Table 2) obtained for the catalyst following calcination at 350 °C which also gave Co_3O_4 XRD peaks even with very weak intensity (Fig. 5). The 781.3 eV peak with the catalyst sample calcined at 570 °C is possibly related to the formation of either $CoTiO_3$, Co_2TiO_4 or both all on the surface of this sample [58,61,71,72], although XRD measurements gave characteristic reflections indicating only the presence of Co_3O_4 even in this catalyst sample. Calcination of CoO_x/TiO_2 catalysts at 400 °C in a flow of pure oxygen for 16 h could give Co $2p_{3/2}$ main peak binding energies near 781.2 ± 0.2 eV, due to the formation of $CoTiO_3$ in addition to Co_3O_4 particles [71]. A 10 wt% CoO_x/TiO_2 catalyst calcined at 450 °C in air for 24 h had a local electronic structure of Co_3O_4, as verified by an extended X-ray absorption fine structure (EXAFS) technique, but an EXAFS spectrum indicating $CoTiO_3$ formation was obtained after calcination at 650 °C for 24 h [74]. Therefore, our XPS and XRD measurements are in reasonable agreement with these earlier XPS and EXAFS studies. Although the 781.3 eV peak binding energy was very close to that for the reference $Co(OH)_2$ (Table 2), it would not be due to this Co species because of both the calcination of 5 wt% CoO_x/TiO_2 at 570 °C prior to being used for XPS measurements and no XRD peaks for $Co(OH)_2$ in this catalyst sample (Fig. 5d). Consequently, the noticeable difference between the XPS spectra of the catalyst samples calcined at 450 and 570 °C, that gave significantly different activities in the oxidation of CO at 100 °C (Figs. 1 and 2), is the value of the binding energies for Co $2p_{3/2}$ main structure.

Based on the previous discussion and the Co $2p_{3/2}$ binding energy values given in Table 2, coupled with the dependence of the catalytic performances on the calcination temperature, it is proposed that five types of model CoO_x species can exist with 5 wt% CoO_x/TiO_2 calcined at different temperatures, particularly 450 and 570 °C, as shown in Fig. 9. Type A, clean Co_3O_4 particles, which are predominantly formed after calcination at 450 °C and highly active for CO oxidation at 100 °C. Type B, Co_3O_4 particles encapsulated completely by Co_nTiO_{n+2}, being produced upon the calcination at 570 °C and having no catalytic performance in this reaction and negligible CO chemisorption. Type C, Co_3O_4 particles covered partially by Co_nTiO_{n+2}, being produced during the calcination at 450 °C and exhibiting a moderate catalytic activity for this oxidation reaction. Both Types D and E, consisting of the respective CoO and Co_nTiO_{n+2} particles, can be eliminated based on XRD measurements in which these Co species were not indicated. The predominant population of the Type A Co_3O_4 nanoparticles in the catalyst after calcination at 450 °C is consistent with the measured binding energy and CO desorption spectrum, and this is in good agreement with earlier studies reporting very high activity of pure Co_3O_4 powders for CO oxidation even at subambient temperatures. The Co $2p_{3/2}$ main peak binding energy of the catalyst consisting predominantly of the Type B Co_3O_4 particles with a large crystallite size of 29 nm would be very similar to that measured with the synthesized Co_nTiO_{n+2} compounds due to such complete encapsulation; however, XRD measurements may give discernable peaks for Co_3O_4 crystallites because of very thin Co_nTiO_{n+2} overlayer on the surface of the Co_3O_4 particles and their crystallite size sufficient to be clearly visible by XRD technique. It is not clear whether the Type C Co_3O_4 particles are present on the titania surface or not. Minute amounts of this Co species may

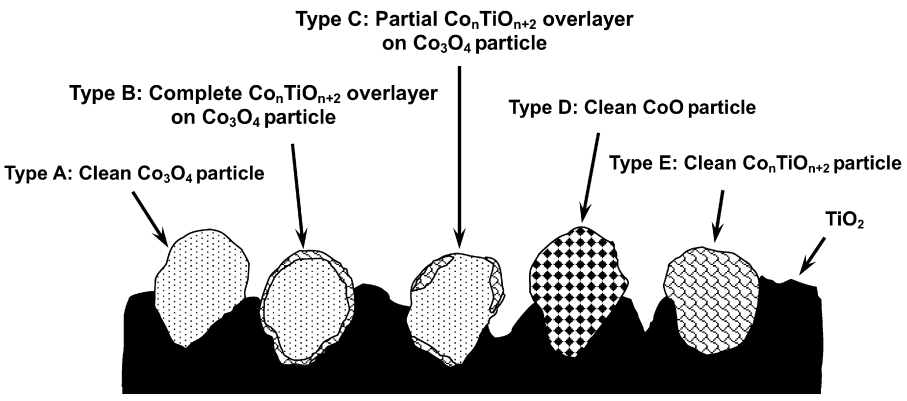

Fig. 9. A proposed model for cobalt oxide species existing with 5 wt% CoO_x/TiO_2 after calcination at different temperatures.

exist with the catalyst calcined at 450 °C since there is no significant difference in the Co $2p_{3/2}$ main peak binding energies between the catalyst sample calcined at 450 °C and the reference Co_3O_4. Consequently, this proposal for the Co species existing with samples of the catalyst after calcination at different temperatures can reasonably explain the dramatic dependence of the catalytic activity for the low-temperature CO oxidation on the calcination temperatures and is consistent with the characterization using TPD, XRD, and XPS measurements.

5. Conclusions

A 5 wt% CoO_x/TiO_2 catalyst is highly active for the oxidation of CO at low temperatures, such as 100 °C, under a purely oxidizing condition, but the extent of CO conversion is strongly dependent on calcination temperatures of this catalyst. The most promising performance was obtained with the catalyst after calcination at 450 °C to form Co_3O_4 nanoparticles highly active for this oxidation reaction. The sample calcined at lower temperatures was less active, and practically zero activity was revealed with a sample of the catalyst, that had been subjected to calcination at 570 °C. These activity dependences on the calcination temperature of the catalyst are consistent with the results acquired by TPD, XRD and XPS measurements. The catalyst after calcination at 450 °C had a 780.2 eV main peak for Co $2p_{3/2}$ and this binding energy was similar to that measured with Co_3O_4 among the reference Co compounds, while the catalyst following calcination at lower temperatures possessed somewhat lower binding energies for Co $2p_{3/2}$ main structure. Not only did the catalyst calcined at 570 °C give a main peak at a Co $2p_{3/2}$ binding energy of 781.3 eV, which was very close to that for Co_nTiO_{n+2} compounds, but the extent of CO chemisorption on this sample also decreased dramatically as measured by TPD. No evidence for CoO and Co_nTiO_{n+2} species was observed in all these catalyst samples, irrespective of calcination temperature, but samples of the catalyst calcined at 350 °C and higher temperatures gave XRD peaks indicating Co_3O_4 formation. Based on these results, the predominant CoO_x species in the catalyst sample after calcination at 450 °C was the Type A clean Co_3O_4 particles, which are highly active for CO oxidation at 100 °C, but the calcination at higher temperatures, such as 570 °C, resulted in the Type B Co_3O_4 crystallites covered completely by very thin Co_nTiO_{n+2} layers that were inactive for this oxidation reaction.

Acknowledgment

A partial grant-in-aid for this study was provided by the Korea Research Foundation via Grant KRF-2006-331-D00108.

References

[1] K. Epping, S. Aceves, R. Bechtold, J. Dec, SAE Technical Paper 2002-01-1923.
[2] M.H. Kim, I.S. Nam, Catalysis 18 (2005) 116.
[3] E. Gulari, C. Guldur, S. Srivannavit, S. Osuwan, Appl. Catal. A 182 (1999) 147.
[4] J. Jansson, A.E.C. Palmqvist, E. Fridell, M. Skoglundh, L. Osterlund, P. Thormahlen, V. Langer, J. Catal. 211 (2002) 387.
[5] H. Gong, J.Q. Hu, J.H. Wang, C.H. Ong, F.R. Zhu, Sens. Actuators B 115 (2006) 247.
[6] S.H. Taylor, G.J. Hutchings, A.A. Mirzaei, Chem. Commun. (1999) 1373.
[7] D.M. Whittle, A.A. Mirzaei, J.S.J. Hargreaves, R.W. Joyner, C.J. Kiely, S.H. Taylor, G.J. Hutchings, Phys. Chem. Chem. Phys. 4 (2002) 5915.
[8] D. Cameron, R. Holliday, D. Thompson, J. Power Sources 118 (2003) 298.
[9] M. Azar, V. Caps, F. Morfin, J.L. Rousset, A. Piednoir, J.C. Bertolini, L. Piccolo, J. Catal. 239 (2006) 307.
[10] B. Schumacher, Y. Denkwitz, V. Plzak, M. Kinne, R.J. Behm, J. Catal. 224 (2004) 449.
[11] G. Marban, A.B. Fuertes, Appl. Catal. B 57 (2005) 43.
[12] A.F. Ghenciu, Curr. Opin. Solid State Mater. Sci. 6 (2002) 389.
[13] A. Martinez-Arias, A.B. Hungria, G. Munuera, D. Gamarra, Appl. Catal. B 65 (2006) 207.
[14] G. Sedmak, S. Hocevar, J. Levec, J. Catal. 213 (2003) 135.
[15] Y. Minemura, M. Kuriyama, S.I. Ito, K. Tomishige, K. Kunimori, Catal. Commun. 7 (2006) 623.
[16] A. Bhave, M. Kraft, F. Mauss, A. Oakley, H. Zhao, SAE Technical Paper 2005-01-0161.
[17] J.R. Linna, R. Stobart, R.P. Wilson, in: Proceedings of the Windsor Workshop 2000 Transportation Fuels, ATF Engine Management Systems, Toronto, Ont., 2000.
[18] R.H. Stanglmaier, C.E. Roberts, SAE Technical Paper 1999-01-3682.
[19] M.H. Kim, I.S. Nam, Korean J. Chem. Eng. 18 (2001) 725.
[20] M. Iwamoto, N. Mizuno, J. Auto. Eng. 207 (1993) 23.
[21] A. Manasilp, E. Gulari, Appl. Catal. B 225 (2004) 489.
[22] S.Y. Chin, O.S. Alexeev, M.D. Amiridis, Appl. Catal. A 286 (2005) 157.
[23] G. Avgouropoulos, T. Ioannides, Ch. Papadopoulou, J. Batista, S. Hocevar, H.K. Matralis, Catal. Today 75 (2002) 157.
[24] Y.J. Mergler, A. van Aalst, J. van Delft, B.E. Nieuwenhuys, J. Catal. 161 (1996) 310.
[25] K.I. Choi, M.A. Vannice, J. Catal. 131 (1991) 1.
[26] M. Haruta, N. Yamada, T. Kobayashi, S. Iijima, J. Catal. 115 (1989) 301.
[27] R.J.H. Grisel, B.E. Nieuwenhuys, J. Catal. 199 (2001) 48.
[28] A. Wolf, F. Schuth, Appl. Catal. A 226 (2002) 1.
[29] F. Moreau, G.C. Bond, A.O. Taylor, Chem. Commun. (2004) 1642.
[30] M. Koudiakov, M.C. Gupta, S. Deevi, Nanotechnology 15 (2004) 987.
[31] M.R. Kim, S.I. Woo, Appl. Catal. A 299 (2006) 52.
[32] R. Burch, J.A. Sullivan, T.C. Watling, Catal. Today 42 (1998) 13.
[33] P. Gelin, L. Urfels, M. Primet, E. Tena, Catal. Today 83 (2003) 45.
[34] K. Ruth, M. Hayes, R. Burch, S. Tsubota, M. Haruta, Appl. Catal. B 24 (2000) L133.
[35] H. Wakita, Y. Kani, K. Ukai, T. Tomizawa, T. Takeguchi, W. Ueda, Appl. Catal. A 283 (2005) 53.
[36] Z. Liu, R. Zhou, X. Zheng, J. Mol. Catal. A 255 (2006) 103.
[37] D.H. Kim, J.E. Cha, Catal. Lett. 86 (2003) 107.
[38] U.R. Pillai, S. Deevi, Appl. Catal. B 64 (2006) 146.
[39] R.C. Reuel, C.B. Bartholomew, J. Catal. 85 (1984) 78.
[40] Y.F. Yu Yao, J. Catal. 33 (1974) 108.
[41] F. Grillo, M.M. Natile, A. Glisenti, Appl. Catal. B 48 (2004) 267.
[42] P. Thormahlen, M. Skoglundh, E. Fridell, B. Andersson, J. Catal. 188 (1999) 300.
[43] Y. Teng, H. Sakurai, A. Ueda, T. Kobayashi, Int. J. Hydrogen Energy 24 (1999) 355.
[44] D.A.H. Cunningham, T. Kobayashi, N. Kamijo, M. Haruta, Catal. Lett. 25 (1994) 257.
[45] Y.J. Mergler, J. Hoebink, B.E. Nieuwenhuys, J. Catal. 167 (1997) 305.
[46] J. Jansson, J. Catal. 194 (2000) 55.
[47] F. Marino, C. Descorme, D. Duprez, Appl. Catal. B 58 (2005) 175.
[48] K. Omata, Y. Kobayashi, M. Yamada, Catal. Commun. 6 (2005) 563.
[49] K. Omata, Y. Kobayashi, M. Yamada, Catal. Commun. 8 (2007) 1.
[50] A. Torncrona, M. Skoglundh, P. Thormahlen, E. Fridell, E. Jobson, Appl. Catal. B 14 (1997) 131.
[51] J. Yan, J. Ma, P. Cao, P. Li, Catal. Lett. 93 (2004) 55.
[52] K. Omata, T. Takada, S. Kasahara, M. Yamada, Appl. Catal. A 146 (1996) 255.

[53] W.S. Epling, P.K. Cheekatamarla, A.M. Lane, Chem. Eng. J. 93 (2003) 61.
[54] M.H. Kim, J.R. Ebner, R.M. Friedman, M.A. Vannice, J. Catal. 208 (2002) 381.
[55] M.H. Kim, K.H. Choo, in: Proceedings of the Fourth International Conference on Environmental Catalysis, Heidelberg, Germany, 2005, Paper # 1237.
[56] M.H. Kim, I.S. Nam, Y.G. Kim, J. Catal. 179 (1998) 350.
[57] M. Shou, K.I. Tanaka, K. Yoshioka, Y. Moro-Oka, S. Nagano, Catal. Today 90 (2004) 255.
[58] Y. Brik, M. Kacimi, M. Ziyad, F. Bozon-Verduraz, J. Catal. 202 (2001) 118.
[59] B.A. Sexton, A.E. Hughes, T.W. Turney, J. Catal. 97 (1986) 390.
[60] B.J. Tan, K.J. Klabunde, P.M.A. Sherwood, J. Am. Chem. Soc. 113 (1991) 855.
[61] R. Oukaci, A.H. Singleton, J.G. Goodwin Jr., Appl. Catal. A 186 (1999) 129.
[62] B. Ernst, S. Libs, P. Chaumette, A. Kiennemann, Appl. Catal. A 186 (1999) 145.
[63] A.Y. Khodakov, J. Lynch, D. Bazin, B. Rebours, N. Zanier, B. Moisson, P. Chaumette, J. Catal. 168 (1997) 16.
[64] C. Arrouvel, H. Toulhoat, M. Breysse, P. Raybaud, J. Catal. 226 (2004) 260.
[65] I.N. Martyanov, K.J. Klabunde, J. Catal. 225 (2004) 408.
[66] J. Alvarez, M.C. Asensio, J.L.G. Fierro (Eds.), Spectroscopic Characterization of Heterogeneous Catalysts, vol. 57, Part A, Elsevier, Amsterdam, 1990 , p. A79 (Chapter 2).
[67] M. Meng, P.Y. Lin, Y.L. Fu, Catal. Lett. 48 (1997) 213.
[68] J. van Elp, J.L. Wieland, H. Eskes, P. Kuiper, G.A. Sawatzky, F.M.F. de Groot, T.S. Turner, Phys. Rev. B 44 (1991) 6090.
[69] K.J. Kim, Y.R. Park, Solid State Commun. 127 (2003) 25.
[70] M. Voß, D. Borgmann, G. Wedler, J. Catal. 212 (2002) 10.
[71] S.W. Ho, J.M. Cruz, M. Houalla, D.M. Hercules, J. Catal. 135 (1992) 173.
[72] F. Morales, F.M.F. de Groot, O.L.J. Gijzeman, A. Mens, O. Stephan, B.M. Weckhuysen, J. Catal. 230 (2005) 301.
[73] A.M. Hilmen, D. Schanke, K.F. Hanssen, A. Holmen, Appl. Catal. A 186 (1999) 169.
[74] K. Tohji, Y. Udagawa, S. Tanabe, T. Ida, A. Ueno, J. Am. Chem. Soc. 106 (1984) 5172.